Carcinogenesis vol.19 no.5 pp.889–896, 1998

Arsenite inhibits mitotic division and perturbs spindle dynamics in HeLa S3 cells

See-Chang Huang[1,2] and Te-Chang Lee[1,3]

[1]Institute of Biomedical Sciences, Academia Sinica and [2]Graduate Institute of Life Sciences, National Defense Medical Center, Taipei, Taiwan, R.O.C.

[3]To whom correspondence should be addressed
Email: bmtcl@ibms.sinica.edu.tw.

Arsenical compounds, known to be human carcinogens, were shown to disturb cell cycle progression and induce cytogenetic alterations in a variety of cell systems. We report here that a 24 h treatment of arsenite induced mitotic accumulation in human cell lines. HeLa S3 and KB cells were most susceptible: 35% of the total cell population was arrested at the mitotic stage after treatment with 5 μM sodium arsenite in HeLa S3 cells and after 10 μM in KB cells. Under a microscope, we observed abnormal mitotic figures in arsenite-arrested mitotic cells, including deranged chromosome congression, elongated polar distance of mitotic spindle, and enhanced microtubule immunofluorescence. The spindle microtubules of arsenite-arrested mitotic cells were more resistant to nocodazole-induced dissolution than those of control mitotic cells. According to turbidity assay, arsenite at concentrations below 100 μM significantly enhanced polymerization of tubulins. Since spindle dynamics play a crucial role in mitotic progression, our results suggest that arsenite-induced mitotic arrest may be due to arsenite's effects on attenuation of spindle dynamics.

Introduction

Epidemiological evidence strongly indicates that chronic exposure to arsenical compounds increases the incidence of skin, lung, liver, bladder and kidney cancer in humans (1–5). However, evidence for arsenic carcinogenicity in experimental animals remains inadequate (1). Due to the lack of an appropriate animal model to study the mechanism of arsenic-induced carcinogenicity, the genotoxic effects of arsenical compounds have been widely studied in numerous *in vitro* systems. Inorganic arsenicals were able to induce chromosome aberrations (6), sister chromatid exchanges (7,8), micronuclei (9–11), aneuploidy (6,12), cell transformation (13) and gene amplification (14), but they failed to induce mutation in specific loci, such as hypoxanthine/guanine phosphoribosyl transferase and Na^+/K^+-ATPase in rodent cells (13).

Arsenite, a trivalent inorganic arsenical, is widely used to study the toxic effects of arsenicals. Arsenite at the concentration of 10 μM induced a radiomimetic delay of cell division in Chinese hamster ovary (CHO*) cells (15). Mitotic indexes were slightly increased in arsenite-treated human peripheral blood lymphocytes (6). Arsenite at relatively high concentrations (>20 μM), like several other heavy metals (e.g. Cd^{2+}, Pb^{2+}, Ni^{2+}), has been shown to severely damage microtubules in mouse 3T3 cells (16,17). We have previously demonstrated that arsenite inhibited the formation of spindle microtubules by treating G2-enriched human fibroblasts or CHO cells with arsenite at the concentration of 100 μM for 2 h (18,19). However, treatment of HeLa S3 cells with arsenite at a sublethal concentration (5 μM) for 24 h resulted in mitotic arrest followed by apoptosis (manuscript in preparation). Although arsenite at high and low concentrations may have different toxic mechanisms, these studies suggest that arsenite may mimic microtubule poisons to interrupt mitotic division.

Cellular microtubules usually form a dynamic polarized network emanating from a microtubule organization centre. At the G2/M transition, cytoplasmic microtubules breakdown and re-organize as more dynamic mitotic spindle (20,21). The dynamic mitotic spindle plays a crucial role in accurate congression and segregation of chromosomes during mitosis. Many chemicals, such as estrogen (22), tamoxifen (23), asbestos (24) and chloral hydrate (25), and many microtubule inhibitors (e.g. colchicine, nocodazole and taxol) (26–28) have been shown to interfere with the assembly and disassembly of mitotic spindle, disrupt chromosome congression, block mitotic exit and induce aneuploidy. The induction of aneuploidy plays an important and possibly essential role in neoplastic development (29). Arsenite may serve as a useful clue for unravelling the mechanism of abnormal mitotic segregation. In this study, experiments were conducted to understand the effects of arsenite on mitotic division and spindle dynamics in HeLa S3 cells.

***Abbreviations**: CHO, Chinese hamster overy cells; HFW, human fibroblasts; HFLF, human foetal lung fibroblasts; PBS, phosphate-buffered saline.

Materials and methods

Cells and cell culture

HeLa S3, HeLa (CCL2), KB, C33A and 293 cells were purchased from American Type Culture Collection (Rockville, MD). Primary human newborn foreskin fibroblasts (HFW) were obtained from Dr W.N.Wen (National Taiwan University, Taiwan) and foetal lung fibroblasts (HFLF) were obtained from Dr M.T.Hsu (Institute of Biomedical Sciences, Academia Sinica). Cells were subcultured twice a week in Dulbecco's minimum essential medium supplemented with 10% heat-inactivated foetal calf serum, 1% L-glutamate, 100 units/ml penicillin, 100 μg/ml streptomycin and 1% non-essential amino acids. The cultures were maintained in a humidified incubator at 37°C with 5% CO_2 and 95% air.

Mitotic index analysis

Logarithmically growing cells were replated at a density of 2.5×10^4 cells per cm^2 in 60-mm dishes 1 day prior to arsenite treatment. Cells were treated with various concentrations of sodium arsenite (0–20 μM) for 24 h. Afterward, the cells, including both rounded-up and attached cells, were harvested by trypsinization, washed once with phosphate-buffered saline (PBS), and then treated with 0.5% KCl for 12 min at room temperature. After centrifugation, the cells were fixed with methanol/acetic acid solution (3:1, v/v). An aliquot of the cell suspension was dropped onto a clean slide, air-dried and stained with a 3% Giemsa solution in Söresen buffer. The mitotic cells which possessed condensed chromosomes were microscopically distinguished from the interphase cells which contained an interphase nucleus. In each culture, at least 200 cells were scored for estimation of mitotic indexes. The mitotic indexes were averaged from three independent experiments.

DNA histogram analysis

After treatment of asynchronous HeLa S3 cells with 5 μM sodium arsenite for 24 h, the rounded-up cells were harvested by a mechanical shake-off

technique and designated as detached cells. The remaining population designated as attached cells was harvested with the aid of trypsinization. The detached and attached cells were separately harvested and fixed with cold 70% ethanol at 4°C overnight. Their cell cycle distribution was analysed by flow cytometry as previously described (30). In brief, the ethanol-fixed cells were centrifuged and resuspended in PBS containing 4 μg/ml propidium iodide, 0.1 mg/ml RNase A and 0.1% Triton X-100, and the DNA content of 10 000 cells was individually analysed with a flow cytometer (FACStar, Becton Dickinson Immunocytometry Systems, Mt View, CA).

Immunoblotting analysis of mitotic regulatory proteins

The cellular levels of c-Mos, cyclin A and cyclin B1 in arsenite (5 μM, 24 h) treated cells were analysed by an immunoblotting technique. In brief, arsenite treated cells were mechanically separated into detached and attached populations, and lysed in 2X SDS-polyacrylamide gel electrophoresis sample buffer (31). Protein concentrations were determined with a Bio-Rad assay kit (Bio-Rad Laboratories, Hercules, CA). After boiling for 5 min, 40 μg of total cellular proteins were electrophoretically separated onto a 12% SDS-polyacrylamide gel and transferred onto nitrocellulose membranes. The membranes were then immunoblotted with c-Mos, cyclin A (Upstate Biotechnology Inc., Lake Placid, NY) or cyclin B1 (Oncogene Research Products, Cambridge, MA) antibodies and the alkaline phosphatase-conjugated secondary antibody as previously described (12). Asynchronous cells and nocodazole-induced (1 μM, 24 h) mitotic cells were included for comparison.

Assay of $p34^{cdc2}$/cyclin B (histone H1) kinase activity

Preparation of cell extracts and assay of $p34^{cdc2}$/cyclin B (histone H1) kinase activity was essentially as described by Juan and Wu (32). Forty micrograms of cell extract were reacted with 1 μg of cyclin B1 antibody. The immunocomplexes were trapped on protein A-conjugated agarose and pelleted by centrifugation. Histone H1 kinase activity was assayed by an addition of 10 μl reaction buffer containing 2.5 μCi [γ-^{32}P]ATP (3000 Ci/mmol) and 10 μg histone H1 and incubated at 37°C for 30 min. The reaction was stopped by mixing with 20 μl of 2X SDS-polyacrylamide gel electrophoresis sample buffer and boiling for 5 min. The supernatants were electrophoretically separated onto a 10% SDS-polyacrylamide gel. The phosphorylated histone H1 was visualized by an autoradiography technique.

Mitotic interference by arsenite

Nocodazole-arrested mitotic cells were used for studying the immediate interference of mitotic division by arsenite. The logarithmically growing cells were briefly incubated with 0.1 μM nocodazole for 4 h. Nocodazole-arrested mitotic cells were harvested by a mechanical shake-off technique, washed once with PBS, and then treated with various concentrations of sodium arsenite (0–50 μM) for 1 or 2 h. The cells were harvested by trypsinization and subjected to mitotic index examination as described above.

Examination of mitotic spindle and chromosome congression

For immunofluorescent staining, the detached mitotic cells were harvested and spun on to glass coverslips with a cytospinner at 1000 rpm for 1 min. The cells on coverslips were fixed with 3.7% phosphate-buffered formaldehyde and 0.1% Triton X-100 for 10 min at room temperature. After washing twice with PBS, the coverslips were incubated with anti-β-tubulin antibody (Sigma, St Louis, MO) diluted 250× in PBS at 37°C for 1 h. At the end of incubation, the coverslips were washed twice with PBS and incubated with FITC-conjugated secondary antibody (1000× dilution in PBS) at 37°C for 30 min. The coverslips were then briefly washed with distilled water and mounted on a slide with GEL/MOUNT™ mounting solution (Biomeda, Foster City, CA). The mitotic spindle was examined under a fluorescence microscope. The polar distance (p.d.) and equator diameter (e.d.) of 20 randomly selected mitotic spindles of each treatment were measured by using an eyepiece micrometer.

A differential staining technique was adopted to simultaneously visualize the mitotic spindle and chromosomes (33). Briefly, the detached mitotic cells were fixed with methanol:acetic acid (3:1, v/v) solution containing 4 mM $MgCl_2$ and 1.5 mM $CaCl_2$ at room temperature. The cells were dropped onto a clean slide and treated with 5% perchloric acid for 24 h before staining with 0.5% Coomassie blue R-250 and 0.5% safranin O in a 10% acetic acid solution.

Disassembly and re-assembly of mitotic spindle in vivo

To study the effects of arsenite on the function of mitotic spindle, their disassembly and re-assembly of arsenite-arrested mitotic cells were compared with that of taxol-arrested and normal mitotic cells. The mitotic cells from logarithmically growing control cultures, arsenite-treated (5 μM, 24 h) and taxol-treated (0.1 μg/ml, 24 h) cultures were harvested by mechanical shake-off and washed once with PBS. For mitotic spindle disassembly assay, the PBS washed mitotic cells were incubated with 20 μM of nocodazole in medium at 37°C. At various time points (0–30 min), an aliquot of cells was fixed with 3.7% phosphate-buffered formaldehyde and 0.1% triton X-100 for 10 min, and immuno-stained with anti-β-tubulin antibody and FITC-conjugated secondary antibody as described above. The disassembly of mitotic spindle was examined under a fluorescence microscope.

For re-assembly assay, the mitotic spindle in control and arsenite-arrested mitotic cells were dissolved by incubation of these cells with ice-cold medium for 1 h. Afterward, the cells were transferred to a 32°C water bath. At various time points (0–20 min), an aliquot of cells was fixed and stained with anti-β-tubulin antibody as described above. The re-assembly of mitotic spindle was examined under a fluorescence microscope. Arsenite at the concentration of 5 μM was continuously presented in the medium during the cold treatment and the spindle re-assembly period at 32°C.

Determination of arsenite accumulation

The logarithmically growing HeLa cells were treated with 5 μM arsenite for 24 h. The detached mitotic cells were harvested by shake-off technique, and the attached cells by trypsinization. After they were washed several times with PBS containing 1 mM EDTA, the arsenic contents were determined with the aid of an atomic absorption spectrophotometer after digestion with nitric acid (34). To estimate the cell volume, the diameters of 30 detached mitotic cells or tryspinized cells were measured under a microscope with an eyepiece micrometer.

Turbidity assay

The *in vitro* microtubule assembly was monitored by light scattering or turbidimetry as described by Lin and Chou (35). Briefly, microtubule proteins were isolated from calf brain by two cycles of temperature-dependent assembly-disassembly in PEM buffer (0.1 M PIPES, pH 6.6, 1 mM EGTA, 1 mM $MgCl_2$). To study the effect of arsenite on microtubule assembly, 1 mM GTP and various concentrations of sodium arsenite were inoculated into the microtubule solution in a cuvette sitting on ice. The reaction was initiated by transferring the cuvette to a Hitachi U-3210 spectrophotometer with a setting at 32°C and the turbidity was continuously recorded at the wavelength of 350 nm. The microtubule polymerization curves were obtained by fitting the data with a polynomial model provided by SigmaPlot (Jandel scientific software, San Rafael, CA) and the initial rate of microtubule polymerization was then estimated at time zero.

Results

Mitotic arrest by arsenite

To examine whether arsenite is a mitotic inhibitor, HeLa S3, HeLa CCL2, KB, HFW, HFLF, C33A and 293 cells were treated with sodium arsenite at a range from 0 to 20 μM. The mitotic indexes were examined by chromosome spreading. A typical field showing the mitotic figures and interphase nuclei under a microscope is presented in Figure 1A. The mitotic indexes of these asynchronous human cell lines in untreated cultures ranged from 2 to 4%. After 24 h incubation, arsenite treatment at concentrations from 3 to 10 μM apparently resulted in mitotic accumulation in these cell lines (Figure 1B). At higher concentrations, the decline of mitotic index may have been due to the toxicity of arsenite at levels too high to allow the cells to move toward mitosis from other cell cycle stages. As shown in Figure 1B, HeLa S3 cells were one of the most sensitive cell lines to arsenite-induced mitotic arrest among the cell lines studied. Treatment of HeLa S3 cells with 5 μM arsenite resulted in 35% cell population arrest at the mitotic stage. HeLa S3 cells were therefore used for further study.

As compared to the control culture (Figure 2A), treatment of HeLa S3 cells with 5 μM sodium arsenite for 24 h remarkably increased the number of detached cells (Figure 2B). Mitotic cells usually round up and detach from the culture dishes. To confirm whether the detached cells were mitotic cells, they were harvested by shake-off technique and subjected to flow cytometric analysis and cytological examination. The DNA histogram of the attached cells (Figure 2D) remained similar to that of the control culture (Figure 2C), but with a slight increase in the S and G2/M population. The mitotic indexes of the control culture and the attached cells were 3 and $<$1%, respectively. However, in the detached cells, the

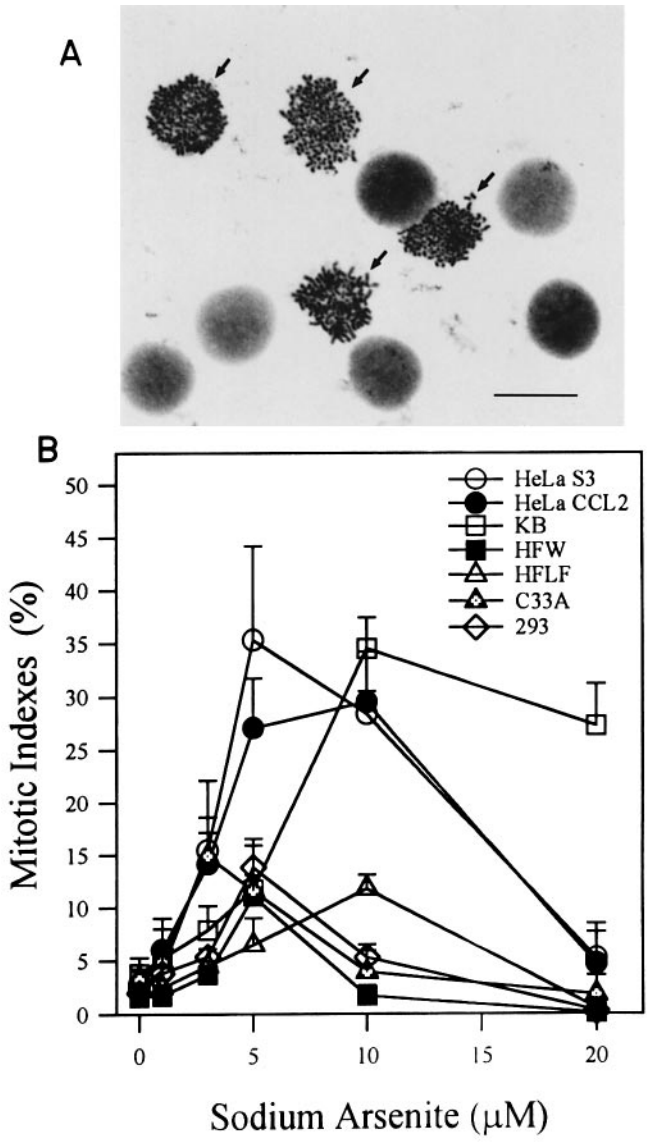

Fig. 1. Mitotic accumulation by arsenite in human cells. (**A**) Microscopic examination of mitotic figures (arrow) and interphase nuclei. HeLa S3 cells were treated with 5 μM sodium arsenite for 24 h, and then prepared by chromosome spreading technique for mitotic index analysis as described in Materials and methods. Bar, 25 μm. (**B**) Human cell lines including HeLa S3, HeLa CCL2, KB, HFW, HFLF, C33A and 293 were treated with various concentrations of sodium arsenite (0–20 μM) for 24 h. At the end of treatment, their mitotic indexes were analysed as described in (A). Bars represent the SD of three independent experiments.

cell population with 4C DNA was 91% and the mitotic index was 90% (Figure 2E). These results indicated that most of the detached cells induced by arsenite treatment were mitotic cells.

Mitotic regulatory proteins

To understand how arsenite arrests mitotic progression, the cellular levels of several mitotic regulatory proteins were analysed by immuno-blotting technique. Arsenite-treated cultures were separated into detached mitotic cells and attached interphase cells by mechanical shake-off. Asynchronous culture and nocodazole-arrested mitotic cells, representing interphase and mitotic controls, were included for comparison. As shown in Figure 3, the electrophoretic profiles of c-Mos, cyclin A and cyclin B in arsenite-arrested mitotic cells were similar to those in nocodazole-arrested mitotic cells, i.e. c-Mos was hyperphosphorylated, cyclin A degraded and cyclin B accumulated. Although c-Mos and cyclin B from the attached interphase cells shared similar profiles with those from the asynchronous control cells, a slight increase of cyclin A was revealed in the arsenite treated attached cells (Figure 3). Other mitotic-associated proteins, such as cdc2, cdk2, cdc25C, MAP kinase kinase (MEK), and protein tyrosine phosphatase 1B also showed no difference between arsenite- and nocodazole-arrested mitotic cells (data not shown). Furthermore, the $p34^{cdc2}$/cyclin B kinase activity monitored by histone H1 phosphorylation was highly increased in both arsenite- and nocodazole-arrested mitotic cells, but was negligible in the control culture. H1 kinase activity was slightly increased in the attached interphase cells in arsenite-treated cultures (Figure 3). These mitotic regulatory protein profiles reflect that the detached cells remained at the mitotic stage.

Mitotic interference

Since nocodazole-arrested mitotic cells were able to complete their division shortly after the drug was removed, they were then used to clarify whether arsenite could directly interfere with mitosis. The nocodazole-arrested mitotic cells were harvested and treated with various concentrations (0 to 50 μM) of arsenite for 1 to 2 h. As shown in Figure 4, when nocodazole-arrested mitotic cells were refed in arsenite-free medium, the mitotic index declined from 85% to 5% within 2 h, indicating that the mitotic cells quickly divided and moved toward interphase. However, by incubating the nocodazole-arrested mitotic cells with arsenite, the decline in mitotic index was inhibited by arsenite following a dose-dependent manner (Figure 4). These results indicated that arsenite could inhibit mitotic exit.

Mitotic spindle and chromosome congression

During mitotic division, the formation of bi-polar spindle and chromosome congression at the spindle equator should be completed prior to anaphase and cell division. The microscopic structure of mitotic spindle and chromosome congression were concurrently examined by immunofluorescent technique using anti-β-tubulin antibody and by differential staining technique. By both techniques, the mitotic spindles were well organized as an oval shape in normal mitotic cells (Figure 5A and C), whereas in arsenite-arrested mitotic cells the shape of mitotic spindles showed a significant elongation (Figure 5B and D). The polar distance (p.d.) and the equator diameter (e.d.) of the mitotic spindle, measured under a fluorescence microscope, were 13.3 ± 1.22 μm and 14 ± 1.41 μm in control mitotic cells, and 16.7 ± 1.69 μm and 14 ± 1.57 μm in arsenite-arrested mitotic cells, respectively. The p.d. of arsenite-arrested mitotic cells was statistically and significantly greater (26%) than that of control mitotic cells ($P < 0.001$, according to Student's *t*-test). The averaged p.d./e.d. ratio in normal mitotic cells was 0.95 ± 0.07 which is very close to a sphere. However, the averaged p.d./e.d. ratio in arsenite-arrested mitotic cells was 1.2 ± 0.16, indicating that their mitotic spindle was spheroid in shape. The distribution of p.d./e.d. ratio is shown in Figure 5E. Furthermore, as shown in Figure 5C and D, the chromosomes were well congregated at the equator in normal mitotic cells, whereas they were scattered around the mitotic spindle in arsenite-arrested mitotic cells.

Disassembly and re-assembly of mitotic spindle

Nocodazole is a microtubule disassembly agent. Treatment of mitotic cells harvested from control cultures (Figure 6A) with

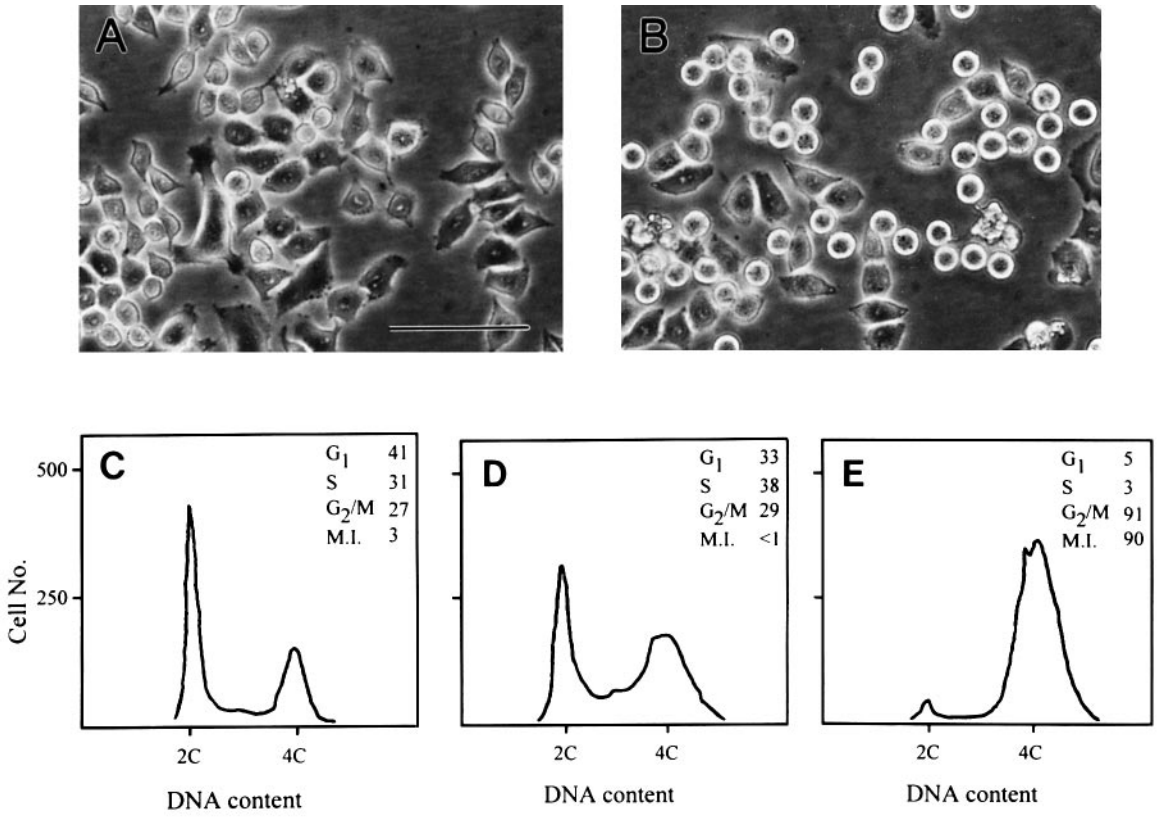

Fig. 2. Cellular morphology and DNA content of arsenite-treated HeLa S3 cells. (A,B) Logarithmically growing HeLa S3 cells were treated with or without 5 μM sodium arsenite for 24 h. The cellular morphology was examined under a phase contrast microscope. (**A**) Control culture. (**B**) Arsenite-treated culture; bar, 25 μm. (C–E) The rounding up cells in arsenite treated culture were detached by a mechanical shake-off technique and the attached cells were harvested by trypsinization. Their DNA content was analysed by flow cytometry as described in Materials and methods. (**C**) Total population of the control culture; (**D**) the attached cell population in arsenite-treated culture; and (**E**) the detached cell population in arsenite-treated culture. The values of cell cycle phase distribution (G1, S and G2/M) and mitotic indexes (M.I.) are presented on the right corner.

20 μM nocodazole at 37°C resulted in disassembly of the mitotic spindle in 2 min (Figure 6B) and complete dissolution in 5 min (Figure 6C). However, the rate of nocodazole-induced spindle disassembly was delayed in arsenite-induced mitotic cells (Figure 6D–H). Residual mitotic spindle remained observable after a 10-min incubation with nocodazole (Figure 6G). For a comparison, taxol, a microtubule stabilizer, was used to arrest mitotic cells. Nocodazole treatment did not disassemble mitotic spindle in taxol-induced mitotic cells (Figure 6I–K).

To analyse the effects of arsenite on the re-assembly of mitotic spindle, the mitotic cells were incubated on ice for 1 h to dissolve the mitotic spindle and were then shifted to a 32°C water bath (Figure 7). As shown in Figure 7A to 7E, the mitotic spindle of untreated control mitotic cells reappeared very quickly. Bi-polar spindle was re-established in 2.5 min (Figure 7B), and the oval shaped mitotic spindle appeared in 20 min (Figure 7E). In fact, anaphase was observed in 30 min and mitotic division was completed in 1–2 h. In arsenite-arrested mitotic cells, the re-assembly of mitotic spindle occurred as quickly as in control mitotic cells. However, the re-assembled mitotic spindle was apparently heavier and the aster fibres around each spindle pole were denser and thicker in arsenite-arrested mitotic cells than those in control mitotic cells (Figure 7F–J). An elongated mitotic spindle was also reformed in arsenite-arrested mitotic cells in 20 min (Figure 7J). Although the mitotic spindle was re-assembled, the arsenite-arrested mitotic cells no longer proceeded to anaphase, even after several hours. They eventually died of apoptotic processes (data not shown).

Cellular arsenite concentrations

As determined by an atomic absorption spectrophotometer, the contents of arsenic in the detached mitotic cells and the attached interphase cells were 10.5 ± 1.9 and 5.7 ± 1.8 ng per 10^6 cells after a treatment with 5 μM for 24 h. With the aid of an eyepiece micrometer, the average diameters of the detached mitotic cells and trypsinized interphase cells were 23.1 ± 4.3 and 16.3 ± 1.8 μm, respectively. Their cell volume was calculated to be 6.5 and 2.3 pl per cell, and the final arsenite concentration in the detached mitotic cells and interphase cells were estimated to be 21.7 ± 3.9 and 25.1 ± 7.9 μM, respectively.

Microtubule assembly in vitro

In vitro microtubule turbidity assay was adopted to further characterize the effects of arsenite on microtubule assembly. Microtubule proteins (0.25 mg/ml) purified from bovine brain were incubated with various concentrations of sodium arsenite (0–200 μM) at 32°C. As shown in Figure 8, arsenite at 20 to 100 μM apparently increased microtubule turbidity in a dose-dependent manner. However, after increasing arsenite concentrations to 200 μM, the enhanced microtubule turbidity was abrogated (Figure 8). By fitting the data with a polynomial model ($r^2 > 0.996$ for all treatments), the initial velocity (v_0) of microtubule polymerization was a biphasic event (Figure 8, inset).

Discussion

In this report, we have demonstrated that sodium arsenite could mimic spindle poisons to induce mitotic arrest in several

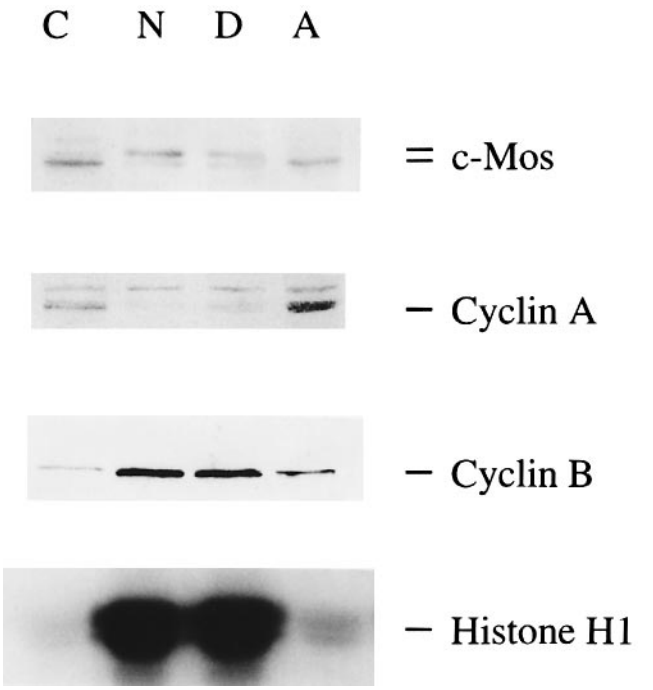

Fig. 3. Electrophoretic profiles of c-Mos, cyclin A and cyclin B, and the activity of $p34^{cdc2}$/cyclin B (histone H1) kinase. The arsenite-treated (5 μM, 24 h) HeLa S3 cells were separated into detached (**lane D**) and attached (**lane A**) populations by mechanical shake-off technique. Nocodazole-arrested (1 μM, 24 h) mitotic cells (**lane N**) and untreated control cells (**lane C**) were included for comparison. After electrophoretic separation, c-Mos, cyclin A, and cyclin B were detected by immuno-blotting technique. Histone H1 kinase activity was assayed using histone H1 and γ-[^{32}P]ATP as substrates as described in Materials and methods.

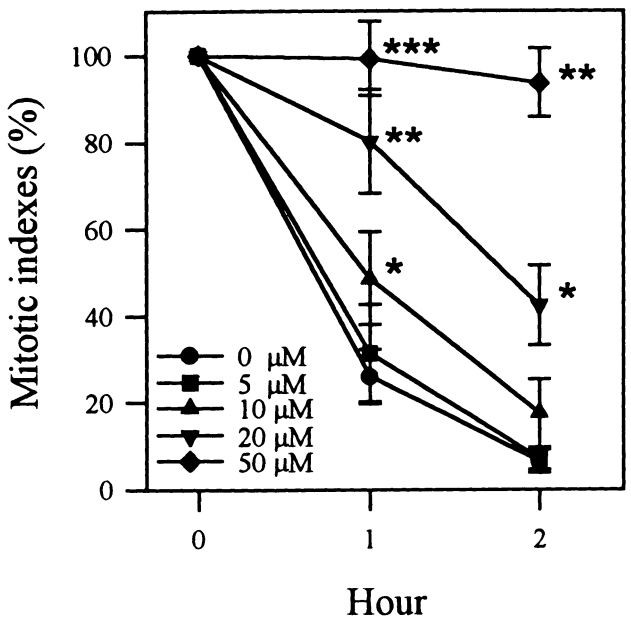

Fig. 4. Inhibition of mitotic exit by arsenite. Nocodazole-arrested (0.1 μM, 4 h) mitotic HeLa S3 cells were harvested by mechanical shake-off technique, washed once with PBS and incubated in medium containing 0 to 50 μM of sodium arsenite for 1–2 h. Their mitotic indexes were then examined as described in Materials and methods. Bars represent the SD of three independent experiments. Asterisks indicate significant difference between arsenite-treated cultures and control culture. $*P < 0.05$; $**P < 0.01$; $***P < 0.001$.

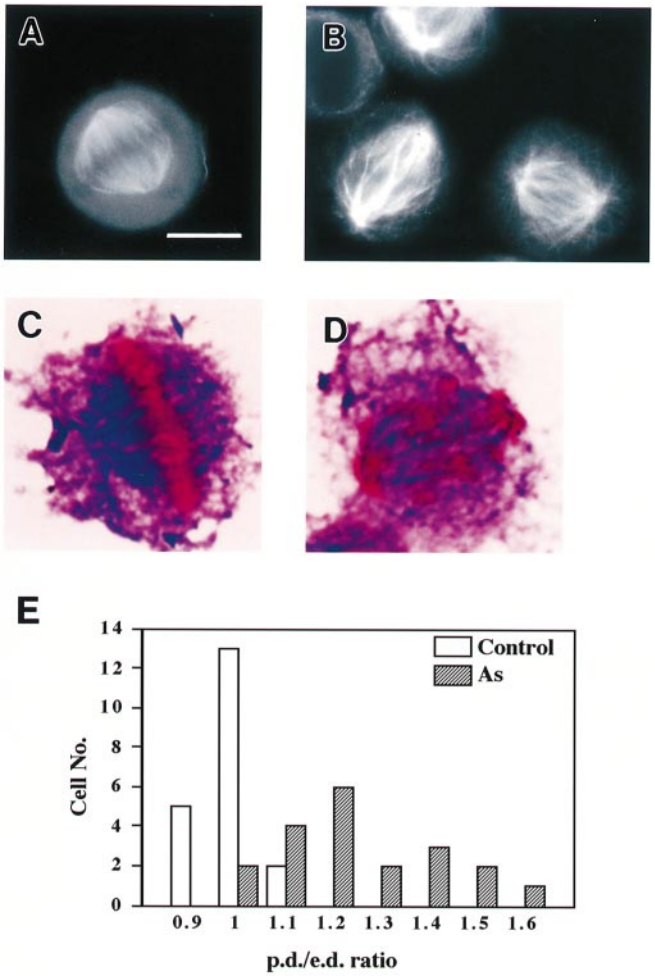

Fig. 5. Spindle morphology and chromosome congression in arsenite arrested mitotic cells. The spindle apparatus and chromosome congression were examined by immunofluorescent technique using anti-β-tubulin antibody (**A,B**) and by differential staining technique (**C,D**) as described in Materials and methods. (A,C) control culture; (B,D) arsenite-treated cultures (5 μM, 24 h), bar, 5 μM. (**E**) The distribution of the ratios of polar distance (p.d.) to equator diameter (e.d.). Twenty mitotic cells stained with anti-β-tubulin antibody and FITC-conjugated secondary antibody were randomly selected from control and arsenite cultures. Their p.d. and e.d were measured under fluorescence microscope.

human cell lines. HeLa S3 and KB cells are the most susceptible lines to arsenite-induced mitotic arrest. Arsenite at 5 and 10 μM resulted in 35% of cells arrested at the mitotic stage in HeLa S3 and KB cells, respectively. The reason why HeLa S3 and KB cells are so susceptible to arsenite-induced mitotic arrest is still unknown. Our present data have shown that arsenite at the concentration used (5 μM, 24 h) did not affect the features of several mitotic regulatory proteins, such as c-Mos, cyclin A and cyclin B, etc. They continued to display their mitotic manifestations in arsenite-arrested mitotic cells. These results indicate that arsenite treatment inhibits mitotic exit. A slight increase in cyclin A levels and H1 kinase activity in arsenite-treated attached cells was possibly due to a slight increase in G2 population.

During mitosis, spindle-assembly checkpoints are activated to ensure accurate segregation of chromosomes. Spindle dynamics play a crucial role in spindle-assembly checkpoints that are required for accurate chromosome segregation (36,37). In our present study, arsenite treatment altered the morphology

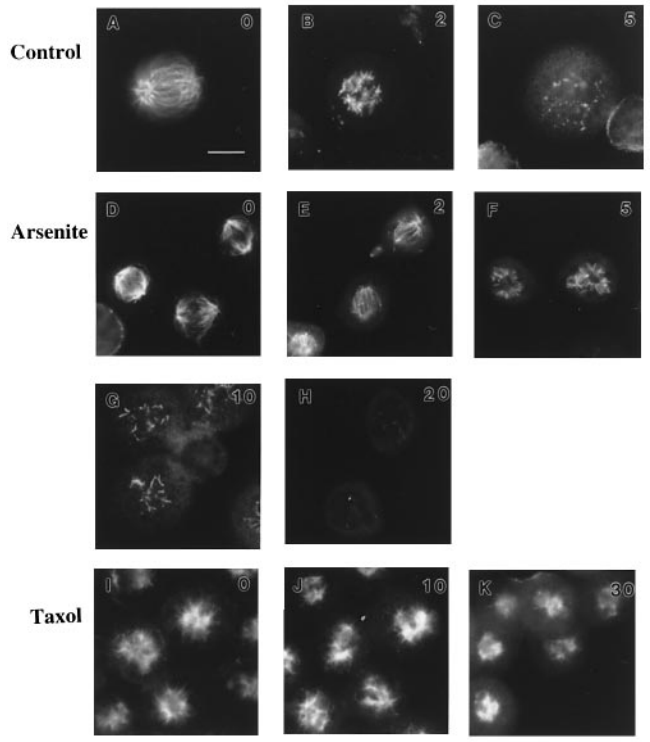

Fig. 6. Retardation of spindle disassembly by nocodazole in arsenite arrested mitotic cells. The mitotic cells from untreated control cultures (**A**–**C**), arsenite-treated (5 μM, 24 h) cultures (**D**–**H**), and taxol-treated (0.1 μg/ml, 24 h; **I**–**K**) cultures were harvested by mechanical shake-off and incubated in medium containing 20 μM of nocodazole at 37°C. At the time (min) indicated on top right, an aliquot of cells was sampled out and immuno-stained with anti-β-tubulin antibody. Bar, 5 μM.

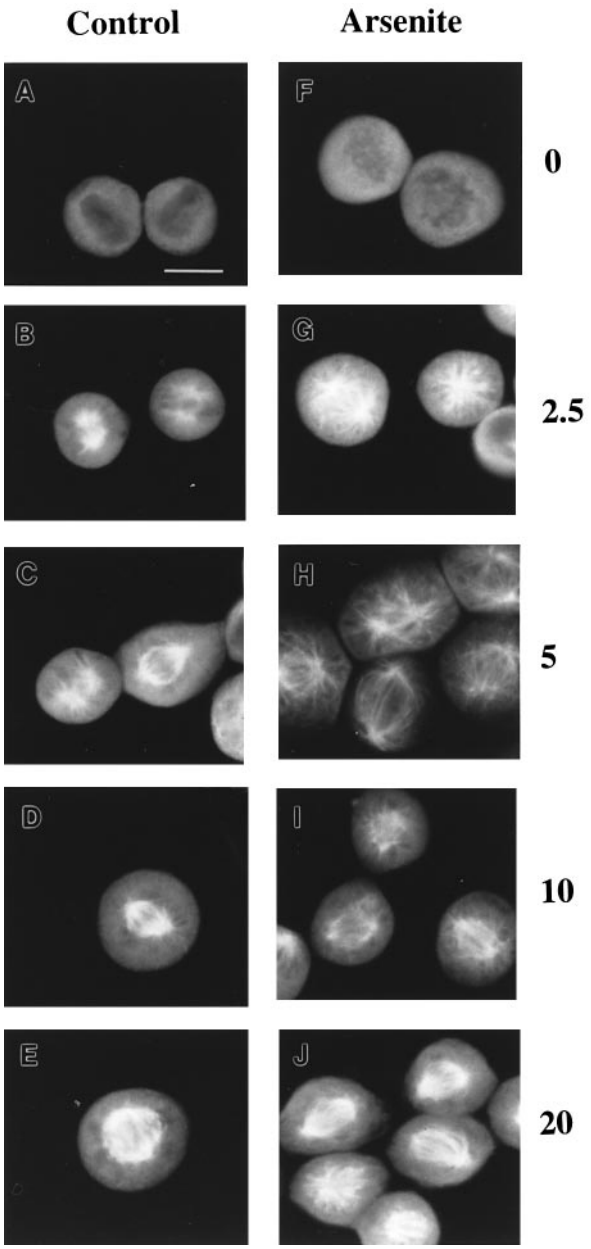

Fig. 7. Spindle re-assembly in arsenite arrested mitotic cells. The mitotic cells from untreated control cultures (**A**–**E**) and arsenite-treated cultures (5 μM, 24 h; **F**–**J**) were incubated on ice for 1 h. Afterward, the cells were transferred to a 32°C water bath. At various time points (min) indicated on right, an aliquot of cells was sampled out and immuno-stained with anti-β-tubulin antibody. Bar, 5 μM.

and the function of mitotic apparatus, such as elongated spindle, thickened aster fibres, and scattered chromosome distribution (Figure 5). We have also demonstrated that nocodazole-induced mitotic spindle disassembly was significantly delayed in arsenite-arrested mitotic cells (Figure 6). These results imply that arsenite treatment may slow down the rate of depolymerization of mitotic spindle. Alternatively, according to the results of re-assembly experiments (Figure 7) and *in vitro* turbidity assay (Figure 8), arsenite may enhance spindle re-assembly. Thus, our results indicate that arsenite at low concentrations attenuates mitotic spindle dynamics instead of disrupting spindle formation. The interference with spindle dynamics by arsenite prevents the onset of anaphase and mitotic exit.

Jordan and colleagues have demonstrated that vinblastine, nocodazole and taxol at low concentrations remarkably increased mitotic indexes without detectable increase in microtubule polymer mass, but significantly attenuated the dynamics of mitotic spindle (27,28). Therefore, the success of mitotic division depends on microtubule dynamic instability. Although arsenite may attenuate the spindle dynamics by moderately stabilizing spindle microtubules, the mechanism of arsenite's effects on spindle dynamics is probably different from those of known spindle poisons such as colchicine, nocodazole and taxol. Colchicine, nocodazole and vinblastine inhibit assembly of mitotic spindle, whereas taxol stabilizes the mitotic spindle. It has been reported that taxol preferentially interacts with the amino-terminal region of β-tubulin (2.5-fold higher than that of α-tubulin; 38,39) and results in increase of subunit spacing and surface-lattice defects (40). In addition, taxol could induce a conformation change of the tubulin dimer that is essential for keeping the protofilaments straight and preventing protofilament-curling at the microtubule ends (40,41).

Arsenite has been known to interact with the thiol group of proteins. Recently, Bhattacharjee and Rosen (42) proposed that arsenite may interact with spatially closed cys-113, cys-172 and cys-422 of ArsA, an ATPase involved in arsenite efflux, to form a trigonal pyramidal motif and thereby activate enzyme activity. Since the primary molecular units of microtubules, α- and β-tubulin, are cysteine rich proteins (12 and 8 cysteine residues, respectively) (43,44), arsenite may interact with these cysteine residuals to form a soft metal-thiol cage and modulate microtubule dynamics. A similar model for interaction of arsenite to cys-12, cys-201 and cys-211 of β-tubulin has been

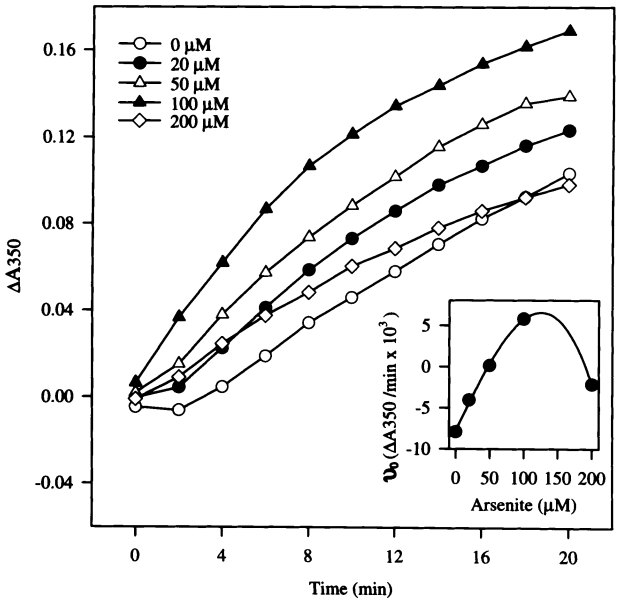

Fig. 8. Effects of arsenite on the microtubule polymerization *in vitro*. Twice-cycled bovine brain microtubule proteins (0.25 mg/ml) were resuspended in PEM buffer (0.1 M PIPES, pH 6.6, 1 mM EGTA, 1 mM $MgCl_2$) supplemented with 1 mM GTP and various concentrations of sodium arsenite (0–500 μM) on ice. The reaction mixture in a cuvette was immediately transfered to a spectrophotometer set at 32°C. The turbidity was continuously recorded at the wavelength of 350 nm. Representative data from one experiment is shown. Inset, the initial polymerization rate (v_0) plotted against arsenite concentrations.

proposed by Hamadeh *et al.* (45). The direct interaction of arsenite to β-tubulin may result in attenuation of spindle dynamics. However, further investigation is needed.

In addition, the spindle-assembly checkpoints may be activated by a signal-transduction cascade. Much evidence has shown that spindle dynamics is regulated through phosphorylation/dephosphorylation of microtubule-associated proteins (46–49). Cyclin-dependent kinase activity may play certain roles in spindle dynamics regulation (50–52). So far, no direct evidence has shown that arsenite can affect the activities of protein kinases and/or phosphatases associated with spindle assembly. However, arsenite treatment results in alteration of phosphorylation profiles of cellular proteins (19,53–56). Therefore, we cannot rule out the possibility that arsenite may attenuate spindle dynamics through a certain cascade of protein phosphorylation/dephosphorylation.

Since arsenite may accumulate in cells, cellular arsenic concentrations may be higher than those in the medium. We determined the cellular arsenic concentration to be 21.7 ± 3.9 μM in arsenite-arrested (5 μM, 24 h) mitotic cells, which was four times higher than that in the medium. At this concentration level, arsenite enhances microtubule polymerization *in vitro* (Figure 8). However, the effects of arsenite on the final polymer mass and the initial rates of microtubule polymerization are biphasic, suggesting that high concentrations of arsenite are too toxic to initiate tubulin polymerization. In fact, like other metal compounds, such as nickel cloride (35), sodium chromate (VI) (57) and methyl mercury (58), arsenite at high concentration disrupts cellular microtubules (17–19).

Recently, Ramirez reported that exposure to arsenite at extremely low concentrations (from 1 nM to 1 μM) for 1 h could disrupt bi-polar mitotic spindles in human peripheral blood lymphocytes and inhibit *in vitro* assembly of microtubules in tubulin purified from newborn mouse brain (59). Furthermore, arsenite did not induce mitotic arrest in peripheral blood lymphocytes (<1%) (6). Whether arsenite may act differently on spindle dynamics in different cell types remains to be further elucidated.

Arsenite has been shown to induce micronuclei, aneuploidy and endoreduplication in human and rodent cells. In our recent report, we have demonstrated that treatment of G2-enriched human fibroblasts with 5 μM arsenite results in mitotic delay and prolongation, and spindle derangement (12). However, 18% of subclones surviving arsenite injury showed one chormosome loss, indicating that arsenite can induce chromosome alterations through disturbance of mitotic events in normal human fibroblasts. The induction of aneuploidy plays an important and essential role in neoplastic development (29). Our present results have shown that arsenite attenuates microtubule dynamics, interrupts chromosome congression, and inhibits mitotic exit in HeLa S3 cells. Since aneuploidy and micronuclei may result from the failure of spindle-assembly checkpoints, it is important to further understand the mechanisms regarding how arsenite disturbs spindle dynamics.

Acknowledgements

We thank Mr Douglas Platt for carefully reading the manuscript. This work was supported by grants from Academia Sinica and the National Science Council (NSC 86-2745-B-001-002), Republic of China.

References

1. IARC (1980) Carcinogenesis of arsenic compounds. *IARC Monograph on Evaluation of Carcinogenic Risks*, vol. 23. IARC, Lyon, pp. 37–141.
2. Brown,K.G. and Chen,C.J. (1995) Significance of exposure assessment to analysis of cancer risk from inorganic arsenic in drinking water in Taiwan. *Risk Anal.*, **15**, 475–484.
3. Chiou,H.Y., Hsueh,Y.M., Liaw,K.F., Horng,S.F., Chiang,M.H., Pu,Y.S., Lin,J.S., Huang,C.H. and Chen,C.J. (1995) Incidence of internal cancers and ingested inorganic arsenic: a seven-year follow-up study in Taiwan. *Cancer Res.*, **55**, 1296–1300.
4. Chen,C.J., Chen,C.W., Wu,M.M. and Kuo,T.L. (1992) Cancer potential in liver, lung, bladder and kidney due to ingested inorganic arsenic in drinking water. *Br. J. Cancer*, **66**, 888–892.
5. Hsueh,Y.M., Cheng,G.S., Wu,M.M., Yu,H.S., Kuo,T.L. and Chen,C.J. (1995) Multiple risk factors associated with arsenic-induced skin cancer: effects of chronic liver disease and malnutritional status. *Br. J. Cancer*, **71**, 109–114.
6. Vega,L., Gonsebatt,M.E. and Ostrosky-Wegman,P. (1995) Aneugenic effect of sodium arsenite on human lymphocytes in vitro: an individual susceptibility effect detected. *Mutat. Res.*, **334**, 365–373.
7. Lee,T.C., Wang-Wuu,S., Huang,R.Y., Lee,K.C. and Jan,K.Y. (1986) Differential effects of pre- and posttreatment of sodium arsenite on the genotoxicity of methyl methanesulfonate in Chinese hamster ovary cells. *Cancer Res.*, **46**, 1854–1857.
8. Jha,A.N., Noditi,M., Nilsson,R. and Natarajan,A.T. (1992) Genotoxic effects of sodium arsenite on human cells. *Mutat. Res.*, **284**, 215–221.
9. Tinwell,H., Stephens,S.C. and Ashby,J. (1991) Arsenite as the probable active species in the human carcinogenicity of arsenic: mouse micronucleus assays on Na and K arsenite, orpiment, and Fowler's solution. *Environ. Hlth Perspect.*, **95**, 205–210.
10. Smith,A.H., Hopenhayn-Rich,C., Warner,M., Biggs,M.L., Moore,L. and Smith,M.T. (1993) Rationale for selecting exfoliated bladder cell micronuclei as potential biomarkers for arsenic genotoxicity. *J. Toxicol. Environ. Hlth*, **40**, 223–234.
11. Wang,T.S. and Huang,H. (1994) Active oxygen species are involved in the induction of micronuclei by arsenite in XRS-5 cells. *Mutagenesis*, **9**, 253–257.
12. Yih,L.H., Ho,I.C. and Lee,T.C. (1997) Sodium arsenite disturbs mitosis and induces chromosome loss in human fibroblasts. *Cancer Res.*, **57**, 5051–5059.

13. Lee,T.C., Oshimura,M. and Barrett,J.C. (1985) Comparison of arsenic-induced cell transformation, cytotoxicity, mutation and cytogenetic effects in Syrian hamster embryo cells in culture. *Carcinogenesis*, **6**, 1421–1426.
14. Lee,T.C., Tanaka,N., Lamb,P.W., Gilmer,T.M. and Barrett,J.C. (1988) Induction of gene amplification by arsenic. *Science*, **241**, 79–81.
15. Gurley,L.R., Walters,R.A., Jett,J.H. and Tobey,R.A. (1980) Response of CHO cell proliferation and histone phosphorylation to sodium arsenite. *J. Toxic. Environ. Hlth*, **6**, 87–105.
16. Chou,I.N. (1989) Distinct cytoskeletal injuries induced by As, Cd, Co, Cr, and Ni compounds. *Biomed. Environ. Sci.*, **2**, 358–365.
17. Li,W. and Chou,I.N. (1992) Effects of sodium arsenite on the cytoskeleton and cellular glutathione levels in cultured cells. *Toxicol. Appl. Pharmacol.*, **114**, 132–139.
18. Gurr,J.R., Lin,Y.C., Ho,I.C., Jan,K.Y. and Lee,T.C. (1993) Induction of chromatid breaks and tetraploidy in Chinese hamster ovary cells by treatment with sodium arsenite during the G2 phase. *Mutat. Res.*, **319**, 135–142.
19. Huang,R.N., Ho,I.C., Yih,L.H. and Lee,T.C. (1995) Sodium arsenite induces chromosome endoreduplication and inhibits protein phosphatase activity in human fibroblasts. *Environ. Mol. Mutagen.*, **25**, 188–196.
20. Karsenti,E., Newport,J., Hubble,R. and Kirschner,M. (1984) Interconversion of metaphase and interphase microtubule arrays, as studied by the injection of centrosomes and nuclei into *Xenopus* eggs. *J. Cell Biol.*, **98**, 1730–1745.
21. Zhai,Y., Kronebusch,P.J., Simon,P.M. and Borisy,G.G. (1996) Microtubule dynamics at the G2/M transition: abrupt breakdown of cytoplasmic microtubules at nuclear envelope breakdown and implications for spindle morphogenesis. *J. Cell Biol.*, **135**, 201–214.
22. Epe,B., Harttig,U., Stopper,H. and Metzler,M. (1990) Covalent binding of reactive estrogen metabolites to microtubular protein as a possible mechanism of aneuploidy induction and neoplastic cell transformation. *Environ. Hlth Perspect.*, **88**, 123–127.
23. Sargent,L.M., Dragan,Y.P., Bahnub,N., Wiley,J.E., Sattler,C.A., Schroeder,P., Sattler,G.L., Jordan,V.C. and Pitot,H.C. (1994) Tamoxifen induces hepatic aneuploidy and mitotic spindle disruption after a single in vivo administration to female Sprague–Dawley rats. *Cancer Res.*, **54**, 3357–3360.
24. Dopp,E., Saedler,J., Stopper,H., Weiss,D.G. and Schiffmann,D. (1995) Mitotic disturbances and micronucleus induction in Syrian hamster embryo fibroblast cells caused by asbestos fibers. *Environ. Hlth Perspect.*, **103**, 268–271.
25. Eichenlaub Ritter,U. and Betzendahl,I. (1995) Chloral hydrate induced spindle aberrations, metaphase I arrest and aneuploidy in mouse oocytes. *Mutagenesis*, **10**, 477–486.
26. Jordan,M.A., Thrower,D. and Wilson,L. (1991) Mechanism of inhibition of cell proliferation by Vinca alkaloids. *Cancer Res.*, **51**, 2212–2222.
27. Jordan,M.A., Thrower,D. and Wilson,L. (1992) Effects of vinblastine, podophyllotoxin and nocodazole on mitotic spindles. Implications for the role of microtubule dynamics in mitosis. *J. Cell Sci.*, **102**, 401–416.
28. Jordan,M.A., Toso,R.J., Thrower,D. and Wilson,L. (1993) Mechanism of mitotic block and inhibition of cell proliferation by taxol at low concentrations. *Proc. Natl Acad. Sci. USA*, **90**, 9552–9556.
29. Weinert,T. and Lydall,D. (1993) Cell cycle checkpoints, genetic instability and cancer. *Semin. Cancer Biol.*, **4**, 129–140.
30. Lee,T.C., Ko,J.L. and Jan,K.Y. (1989) Differential cytotoxicity of sodium arsenite in human fibroblasts and Chinese hamster ovary cells. *Toxicology*, **56**, 289–299.
31. Laemmli,U.K. (1970) Cleavage of structural proteins during the assembly of the head of bacteriophage T4. *Nature*, **227**, 680–685.
32. Juan,C.C. and Wu,F.Y. (1993) Vitamin K3 inhibits growth of human hepatoma HepG2 cells by decreasing activities of both p34cdc2 kinase and phosphatase. *Biochem. Biophys. Res. Commun.*, **190**, 907–913.
33. Wissinger,W.L., Estervig,D.N. and Wang,R.J. (1981) A differential staining technique for simultaneous visualization of mitotic spindle and chromosomes in mammalian cells. *Stain. Technol.*, **56**, 221–226.
34. Huang,R.N. and Lee,T.C. (1996) Arsenite efflux is inhibited by verapamil, cyclosporin A, and GSH-depleting agents in arsenite-resistant Chinese hamster ovary cells. *Toxicol. Appl. Pharmacol.*, **141**, 17–22.
35. Lin,K.C. and Chou,I.N. (1990) Studies on the mechanisms of Ni2(+)-induced cell injury: I. Effects of Ni^{2+} on microtubules. *Toxicol. Appl. Pharmacol.*, **106**, 209–221.
36. Wells,W.A. (1996) The spindle-assembly checkpoint: aiming for perfect mitosis, every time. *Trends Cell Biol.*, **6**, 228–234.
37. Rudner,A.D. and Murray,A.W. (1996) The spindle assembly checkpoint. *Curr. Opin. Cell Biol.*, **8**, 773–780.
38. Combeau,C., Commercon,A., Mioskowski,C., Rousseau,B., Aubert,F. and Goeldner,M. (1994) Predominant labeling of beta- over alpha-tubulin from porcine brain by a photoactivatable taxoid derivative. *Biochemistry*, **33**, 6676–6683.
39. Rao,S., Krauss,N.E., Heerding,J.M., Swindell,C.S., Ringel,I., Orr, G.A. and Horwitz,S.B. (1994) 3′-(p-azidobenzamido)taxol photolabels the N-terminal 31 amino acids of beta-tubulin. *J. Biol. Chem.*, **269**, 3132–3134.
40. Arnal,I. and Wade,R.H. (1995) How does taxol stabilize microtubules? *Curr. Biol.*, **5**, 900–908.
41. Hyman,A.A., Chretien,D., Arnal,I. and Wade,R.H. (1995) Structural changes accompanying GTP hydrolysis in microtubules: information from a slowly hydrolyzable analogue guanylyl-(alpha,beta)-methylene-diphosphonate. *J. Cell Biol.*, **128**, 117–125.
42. Bhattacharjee,H. and Rosen,B.P. (1996) Spatial proximity of Cys113, Cys172, and Cys422 in the metalloactivation domain of the ArsA ATPase. *J. Biol. Chem.*, **271**, 24465–24470.
43. Krauhs,E., Little,M., Kempf,T., Hofer Warbinek,R., Ade,W. and Ponstingl,H. (1981) Complete amino acid sequence of beta-tubulin from porcine brain. *Proc. Natl Acad. Sci. USA*, **78**, 4156–4160.
44. Ponstingl,H., Krauhs,E., Little,M. and Kempf,T. (1981) Complete amino acid sequence of alpha-tubulin from porcine brain. *Proc. Natl Acad. Sci. USA*, **78**, 2757–2761.
45. Hamadeh,H., Lee,E., Vargas,M., Rasmussen,R.E., Meacher,D.M. and Menzel,D.E. (1997) High affinity arsenic binding proteins in human lymphocytes and lymphoblastoid cells. *Workshop on Arsenic: health effects, mechanisms of actions, and research issues*. Hunt Valley, MD.
46. Blangy,A., Lane,H.A., d'Herin,P., Harper,M., Kress,M. and Nigg,E.A. (1995) Phosphorylation by p34cdc2 regulates spindle association of human Eg5, a kinesin-related motor essential for bipolar spindle formation *in vivo*. *Cell*, **83**, 1159–1169.
47. Gabrielli,B.G., De Souza,C.P., Tonks,I.D., Clark,J.M., Hayward,N.K. and Ellem,K.A. (1996) Cytoplasmic accumulation of cdc25B phosphatase in mitosis triggers centrosomal microtubule nucleation in HeLa cells. *J. Cell Sci.*, **109**, 1081–1093.
48. Ookata,K., Hisanaga,S., Bulinski,J.C., Murofushi,H., Aizawa,H., Itoh,T.J., Hotani,H., Okumura,E., Tachibana,K. and Kishimoto,T. (1995) Cyclin B interaction with microtubule-associated protein 4 (MAP4) targets p34cdc2 kinase to microtubules and is a potential regulator of M-phase microtubule dynamics. *J. Cell Biol.*, **128**, 849–862.
49. Preuss,U., Doring,F., Illenberger,S. and Mandelkow,E.M. (1995) Cell cycle-dependent phosphorylation and microtubule binding of tau protein stably transfected into Chinese hamster ovary cells. *Mol. Biol. Cell*, **6**, 1397–1410.
50. Verde,F., Labbe,J.C., Doree,M. and Karsenti,E. (1990) Regulation of microtubule dynamics by cdc2 protein kinase in cell-free extracts of *Xenopus* eggs. *Nature*, **343**, 233–238.
51. Verde,F., Dogterom,M., Stelzer,E., Karsenti,E. and Leibler,S. (1992) Control of microtubule dynamics and length by cyclin A- and cyclin B-dependent kinases in *Xenopus* egg extracts. *J. Cell Biol.*, **118**, 1097–1108.
52. Wheatley,S.P., Hinchcliffe,E.H., Glotzer,M., Hyman,A.A., Sluder,G. and Wang,Y. (1997) CDK1 inactivation regulates anaphase spindle dynamics and cytokinesis *in vivo*. *J. Cell Biol.*, **138**, 385–393.
53. Cobo,J.M., Valdez,J.G. and Gurley,L.R. (1995) Inhibition of mitotic-specific histone phosphorylation by sodium arsenite. *Toxicol. In Vitro*, **9**, 459–465.
54. Guy,G.R., Cairns,J., Ng,S.B. and Tan,Y.H. (1993) Inactivation of a redox-sensitive protein phosphatase during the early events of tumor necrosis factor/interleukin-1 signal transduction. *J. Biol. Chem.*, **268**, 2141–2148.
55. Robaye,B., Hepburn,A., Lecocq,R., Fiers,W., Boeynaems,J.M. and Dumont,J.E. (1989) Tumor necrosis factor-alpha induces the phosphorylation of 28 kDa stress proteins in endothelial cells: possible role in protection against cytotoxicity? *Biochem. Biophys. Res. Commun.*, **163**, 301–308.
56. Trigon,S. and Morange,M. (1995) Different carboxyl-terminal domain kinase activities are induced by heat-shock and arsenite. Characterization of their substrate specificity, separation by Mono Q chromatography, and comparison with the mitogen-activated protein kinases. *J. Biol. Chem.*, **270**, 13091–13098.
57. Nijs,M. and Kirsch Volders,M. (1986) Induction of spindle inhibition and abnormal mitotic figures by Cr(II), Cr(III) and Cr(VI) ions. *Mutagenesis*, **1**, 247–252.
58. Graff,R.D., Philbert,M.A., Lowndes,H.E. and Reuhl,K.R. (1993) The effect of glutathione depletion on methyl mercury-induced microtubule disassembly in cultured embryonal carcinoma cells. *Toxicol. Appl. Pharmacol.*, **120**, 20–28.
59. Ramirez,P. (1997) Disruption of microtubule assembly and spindle formation as a mechanism for the induction of aneuploid cells by sodium arsenite and vanadium pentoxide. *Mutat. Res.*, **386**, 291–298.

Received on November 3, 1997; revised on January 6, 1998; accepted on January 6, 1998